

Batch size invariant Adam

Xi Wang

Manning College of Information and Computer Sciences
University of Massachusetts Amherst

xwang3@cs.umass.edu

Laurence Aitchison

Department of Computer Science
University of Bristol

laurence.aitchison@bristol.ac.uk

Abstract

We propose a batch size invariant version of Adam, for use in large-scale, distributed settings, in which the MINI-batch is divided into MICRO-batches which are distributed among worker nodes. For the v term, standard Adam first computes the average over MICRO-batch gradients, then squares, while in the batch size invariant Adam proposed here, we first square the MICRO-batch gradients, then average. Previous work (e.g. Malladi et al. 2022) used an alternative approach that involved a square-root scaling of the learning rate, but this approach requires strong assumptions to work; in particular that the gradient variance dominates the square of the expected gradient. In contrast, the approach proposed here gives batch size invariance without this assumption. We confirm that in practice our scheme gives batch size invariance in a much larger range of scenarios than the previous approach.

1 Introduction

Adam (Kingma & Ba, 2014) and Adam (Loshchilov & Hutter, 2017) are state-of-art optimizers, commonly used for LLM pretraining runs (e.g. Zhang et al., 2022; Touvron et al., 2023). Given the huge investments in these pretraining runs, it is critical to understand how to tune the hyperparameters of Adam¹. However, as with most optimization algorithms, setting the Adam hyperparameters is difficult. As an example of this, we might want to tune the hyperparameters in smaller-scale settings and transfer those hyperparameters to a single, very large-scale training run. However, to do that effectively, we need our optimization to behave in the same way for any MINI-batch size. This property, which we call batch size invariance, can be achieved straightforwardly in SGD, by scaling the learning rate linearly with the batch size (i.e. $\eta \propto B$) (Krizhevsky, 2014; Stephan et al., 2017; Goyal et al., 2017; Smith & Le, 2017; Smith et al., 2017; Ma et al., 2018; Golmant et al., 2018; McCandlish et al., 2018; Zhang et al., 2019; Shallue et al., 2019). However, for modern adaptive optimizers such as Adam (Kingma & Ba, 2014; Loshchilov & Hutter, 2017), it is more difficult to achieve batch size invariance.

To understand the key barrier to obtaining truly batch size invariant Adam, we need to look at the Adam update rule,

$$\Delta w_t = -\eta \frac{\hat{m}_t}{\sqrt{\hat{v}_t + \epsilon}}. \quad (1)$$

The key term here is \hat{v}_t , which is a debiased, exponential moving average estimate of the raw second moment of the gradient, $E[(g')^2]$ (here, the expectation is over randomness in the choice of datapoints incorporated in the MINI-batch, and we use g' for the MINI-batch gradient as we will use g for the MICRO-batch gradient later in the manuscript). Of course, the raw second moment is the sum of the mean-squared gradient, $E[g']^2$, and the variance of the gradient, $\text{Var}[g']$. The key issue is that the variance of the MINI-batch gradient depends on the MINI-batch size, $\text{Var}[g'] \propto 1/B$ (Granzio et al., 2022; Malladi et al., 2022; Hilton et al., 2022). There

¹We will use Adam to denote both Adam and AdamW for the rest of the manuscript, as our method can be applied.

is therefore an inevitable MINI-batch size dependence in \hat{v}_t , which appears as a change in the effective learning rate, $\eta/(\sqrt{\hat{v}_t} + \epsilon)$.

Recent work suggested correcting for these effects by tweaking the learning rate, η (Granzio et al., 2022; Malladi et al., 2022; Hilton et al., 2022). In particular, they proposed a square-root scaling (i.e. $\eta \propto \sqrt{B}$). However, for this square-root scaling to be valid, strong assumptions need to hold, namely that $\text{Var}[g']$ “dominates” (i.e. is much bigger than) $\text{E}[g']^2$. Of course, this can hardly be guaranteed to hold. In fact, there are two settings where this assumption might break down. First, close to initialization, where $\text{E}[g']$ will be large. Second, as the batch size gets very large (e.g. in large LLM pretraining runs), we would expect $\text{Var}[g'] \propto 1/B$ to become small.

We take a different approach to batch size invariance in Adam, by modifying the Adam updates themselves to eliminate the batch size dependence at source. In particular, we consider a large-scale setting in which a MINI-batch is split into a number of MICRO-batches, which may be distributed among worker nodes. Standard Adam computes the average gradient (across MICRO-batches), then squares. In contrast, we consider an alternative scheme, which first squares the MICRO-batch gradients, then averages across MICRO-batches. We prove that this alternative scheme is batch size invariant under much weaker assumptions. In particular, we do not need the gradient variance to dominate the expectation. We just need sufficiently small updates (e.g. learning rates), which is required by Malladi et al. (2022) anyway, and is just the Adam analogue of the critical batch size in SGD (Ma et al., 2018; Golmant et al., 2018; McCandlish et al., 2018; Zhang et al., 2019; Shallue et al., 2019).

2 Related work

The closest prior work is Granzio et al. (2022), Malladi et al. (2022) and Hilton et al. (2022), as they propose an alternative approach to obtaining batch size invariant Adam by scaling the learning rate to try to post-hoc correct for changes in the effective learning rate, $\eta/(\sqrt{\hat{v}} + \epsilon)$, caused by changes in \hat{v} . In contrast, we propose to eliminate changes in the effective learning rate at source, by proposing a modification to Adam updates. There are three key differences between our approach and this prior work. First, our approach gives a linear scaling of the learning rate, $\eta \propto B$, while the prior work proposes a square-root scaling, $\eta \propto \sqrt{B}$ (this is not a contradiction: both are correct in their respective setups). Second, our theoretical approaches are radically different. In particular, Malladi et al. (2022) use stochastic differential equations. In particular, they take the choice of datapoints in the MINI-batch to be random, and they consider the updates to be random variables. In contrast, in our actual proof (Appendix C), we consider the choice of datapoints in the MINI-batches as fixed, and thus the updates become deterministic. Instead, we ask: if we give the same set of datapoints to two optimizers, in what settings are the resulting weight updates exactly equivalent? Third, our approach gives batch size invariance under much weaker assumptions. In particular, we do not need the gradient variance to dominate the expectation, we only need the updates to be sufficiently small (which is required by Malladi et al. (2022) anyway).

It turns out that this requirement for the updates to be sufficiently small is also encountered in SGD, where it is understood as a critical batch size (Ma et al., 2018). Notably, this work assumes takes $\eta \propto B$ so a critical batch size is intimately related to a critical learning rate. Shallue et al. (2019) introduced the term “perfect” scaling for the region in which training is batch size invariant and studied the effect of e.g. architectures on the critical batch size. The dependence of the critical batch size on dataset (Golmant et al., 2018), gradient noise scale (McCandlish et al., 2018) and curvature Zhang et al. (2019). We observe a similar threshold for batch size invariant Adam (Fig. 2), though in our plots it is most straightforwardly interpreted as a critical learning rate.

The notion of computing the squared gradients for MICRO-batches was also proposed in Zhang et al. (2023), albeit in a very different context. In particular, they were trying to do Adam on large MINI-batches in memory constrained, single-node settings. They therefore considered splitting the MINI-batch into MICRO-batches, and aggregating gradients across the MICRO-batch. They found that they were able to reduce memory consumption by directly aggregating squared MICRO-batch gradients, rather than by aggregating gradients and squaring at the end. However, given common results that smaller batches tend to work better (e.g. Keskar et al., 2016), it is not clear why you would do aggregate across MICRO-batches on a single node: why

Symbol	Description
κ	Number of MICRO-batches in a MINI-batch.
w_t	Parameter values after consuming t MICRO-batch.
$g_t(w)$	Gradient for the t th MICRO-batch evaluated at w .
η	Learning rate.
(γ_1, γ_2)	EMA parameters (related to β_1 and β_2 , Eq. 2).
λ	Weight decay coefficient.

Algorithm 1 MICRO Adam (i.e. standard Adam applied to MICRO-batches)

```

while not converged do
   $m_t = (1 - \gamma_1)m_{t-1} + \gamma_1 g_t(w_{t-1})$ 
   $v_t = (1 - \gamma_2)v_{t-1} + \gamma_2 g_t^2(w_{t-1})$ 
   $\hat{m}_t = \frac{m_t}{1 - \beta_1(\gamma_1)^t}$ 
   $\hat{v}_t = \frac{v_t}{1 - \beta_2(\gamma_2)^t}$ 
   $w_t = (1 - \eta\lambda)w_{t-1} - \eta \frac{\hat{m}_t}{\sqrt{\hat{v}_t + \epsilon}}$ 
end while

```

Algorithm 2 Standard Adam applied to MINI-batches.

```

while not converged do
   $m_t = (1 - \gamma'_1)m_{t-\kappa} + \gamma'_1 \frac{1}{\kappa} \sum_{k=1}^{\kappa} g_{t-k+\kappa}(w_{t-\kappa})$ 
   $v_t = (1 - \gamma'_2)v_{t-\kappa} + \gamma'_2 \left( \frac{1}{\kappa} \sum_{k=1}^{\kappa} g_{t-k+\kappa}(w_{t-\kappa}) \right)^2$ 
   $\hat{m}_t = \frac{m_t}{1 - \beta_1(\gamma'_1)^{t/\kappa}}$ 
   $\hat{v}_t = \frac{v_t}{1 - \beta_2(\gamma'_2)^{t/\kappa}}$ 
   $w_t = (1 - \eta'\lambda)w_{t-\kappa} - \eta' \frac{\hat{m}_t}{\sqrt{\hat{v}_t + \epsilon}}$ 
end while

```

Algorithm 3 Batch size invariant Adam applied to MINI-batches.

```

while not converged do
   $m_t = (1 - \gamma'_1)m_{t-\kappa} + \gamma'_1 \frac{1}{\kappa} \sum_{k=1}^{\kappa} g_{t-k+\kappa}(w_{t-\kappa})$ 
   $v_t = (1 - \gamma'_2)v_{t-\kappa} + \gamma'_2 \frac{1}{\kappa} \sum_{k=1}^{\kappa} g_{t-k+\kappa}^2(w_{t-\kappa})$ 
   $\hat{m}_t = \frac{m_t}{1 - \beta_1(\gamma'_1)^{t/\kappa}}$ 
   $\hat{v}_t = \frac{v_t}{1 - \beta_2(\gamma'_2)^{t/\kappa}}$ 
   $w_t = (1 - \eta'\lambda)w_{t-\kappa} - \eta' \frac{\hat{m}_t}{\sqrt{\hat{v}_t + \epsilon}}$ 
end while

```

not just apply Adam updates to the MICRO-batches? This is confirmed by our results, which show that as updates get too large, and invariance breaks down and smaller batches converge faster (Fig. 2).

Importantly, Zhang et al. (2023) is entirely focused on reducing memory consumption: they do not consider batch size invariance, and such, their proposed algorithm is not batch size invariant. In particular, they consider reducing memory consumption by taking a fixed-size MINI-batch and splitting it into an increasingly large number of MICRO-batches. Of course, as we have more MICRO-batches, each MICRO-batch gets smaller, so the variance of the MICRO-batch gradient estimate gets larger, so \hat{v} will increase and the effective learning rate will fall. Our contribution is therefore entirely orthogonal: establishing that a particular variant of Adam with a particular choice of hyperparameter scaling is invariant to batch size for small enough updates.

That said, the key insight in Zhang et al. (2023) is that you can avoid the memory cost of explicitly accumulating the average gradient by immediately incorporating the MICRO-batch gradients into m_t and the MICRO-batch square gradients into v_t (which is possible in Alg. (3) as the m_t and v_t updates are just sums over MICRO-batches). While Zhang et al. (2023) did not consider the multi-node setting, the key insight holds true in multi-node settings for the server that aggregates gradient updates. In particular, this server again does not need to retain a gradient accumulator, but can just accumulate directly into m_t and v_t . This raises

the prospect of a potential memory saving of 25% at the server (in standard Adam, we need to accumulate four quantities for each parameter, g'_t , m_t , v_t and w_t , while if you use squared MICRO-batch gradients, you only need m_t , v_t and w_t). That raises the tantalising prospect that the batch size invariant Adam considered here is also more efficient in practice in large-scale distributed settings.

We frame our proposal in terms of MICRO-batches computed on separate workers, as that makes it easy to compute the squared gradient for the MICRO-batch on a worker. However, our proposal can also be used in the single-worker setting. For instance, it would be possible to treat each datapoint as a MICRO-batch, and compute the sum of squared gradients for individual datapoints using techniques from [Dangel et al. \(2020\)](#) (which critically avoid needing to materialise the full tensor of individual datapoint gradients, which has an impractically large size of $B \times$ number of parameters).

3 Methods

To set the context, we introduce the concept of MICRO-batch. In particular, we assume a MINI-batch of B samples can be equally split into κ MICRO-batches, and then we aggregate κ sets of gradient computed at *different* microbatches under the *same* parameter values for the actual parameter updates. The idea of MICRO-batch is widely adopted in the training of deep networks, e.g. MICRO-batching facilitates larger MINI-batch sizes under constrained memory by enabling gradient accumulation and supports data parallelism through distributing MICRO-batches across workers for parallel gradient computation. However, our focus diverges from these applications; we leverage MICRO-batching to explore how optimization algorithms are influenced by MINI-batch size, i.e. value of κ . Notice that, we assume a *fixed* MICRO-batch size through the analysis and we will use batch size to denote the *MICRO-batch* size in later paragraphs.

We begin by writing down standard Adam updates applied to individual MICRO-batches (denoted t) (Alg. 1). Here, $g_t(w)$ is the gradient of the objective for the t th MICRO-batch. Note that we have written Adam here in a slightly unusual parameterization, using,

$$\beta_1(\gamma_1) = 1 - \gamma_1 \qquad \beta_2(\gamma_2) = 1 - \gamma_2 \qquad (2)$$

as the scalings we derive later on are much more simply expressed in terms of γ_1 and γ_2 than in terms of β_1 and β_2 . Note that we can recover Adam from AdamW by setting $\lambda = 0$, and incorporating any AdamW weight decay into the objective.

Standard Adam updates (Alg. 2) are performed on a MINI-batch, formed by merging κ MICRO-batches. Importantly, to write down these merged, updates we continue to take t to be *MICRO-batches*, rather than steps or MINI-batches. Of course, each update of standard Adam consumes a single MINI-batch consisting of κ MICRO-batches. Thus, if we start at $w_{t-\kappa}$ then a single step of standard Adam will consume κ MICRO-batches, taking us to w_t . Another step consumes another κ MICRO-batches, taking us to $w_{t+\kappa}$. Thus, while t indexes the number of MICRO-batches, t/κ indexes optimizer steps. This unusual convention has the key benefit that the time indices in standard Adam remains aligned with the time indices in MICRO Adam (Alg. 1), which will be important as we will be assessing equivalence between MICRO Adam and standard Adam or batch size invariant Adam. However, this notation does have the disadvantage that it modifies slightly the form of the debiasing equations (see the powers of steps = t/κ in the expressions for \hat{m} and \hat{v} in Alg. (2) and Alg. (3)).

Batch size dependence in standard Adam. A standard Adam update (Alg. 2) applies to a *MINI-batch* formed by merging κ MICRO-batches. However, the arguments given in the introduction indicate that standard Adam is not batch size invariant. By “batch size invariant”, we mean an algorithm for which, in some sensible limit, a single update on a MINI-batch formed of κ MICRO-batches is equivalent to κ update steps of MICRO Adam on the underlying MICRO-batches (Alg. 1). To see that standard Adam (Alg. 2) is not batch size invariant, we consider the \hat{v}_t terms in the various algorithms. For MICRO Adam (Alg. 1), \hat{v}_t is an exponential moving average of the raw second moment of the *MICRO-batch* gradients,

$$\text{E} [g_t^2(w_{t-1})] = \text{E} [g]^2 + \text{Var} [g]. \qquad (3)$$

where $\mathbb{E}[g]$ and $\text{Var}[g]$ is the mean and variance of MICRO-batch gradients. In contrast, for standard Adam (Alg. 2), \hat{v}_t is an exponential moving average of the raw second moment of the *minibatch* gradients

$$\mathbb{E}\left[\left(\frac{1}{\kappa}\sum_{k=1}^{\kappa}g_{t-k+\kappa}(w_{t-\kappa})\right)^2\right] = \mathbb{E}[g]^2 + \frac{1}{\kappa}\text{Var}[g]. \quad (4)$$

Critically, as we have more MICRO-batches, κ , in the MINI-batch, we get a better estimate of the gradient and hence the variance term falls. And as the effective learning rate, $\eta/(\sqrt{\hat{v}_t} + \epsilon)$ depends on \hat{v}_t , we can see that the effective learning rate depends unavoidably on the batch size.

Batch size invariant Adam. We therefore consider a batch size invariant version of Adam (Alg. 3) in which the red term is the average over squared MICRO-batch gradients (as opposed to standard Adam, where the red term is the square of average MICRO-batch gradients). Thus, in batch size invariant Adam (Alg. 3), just like in MICRO Adam (Alg. 1), \hat{v} estimates the expected raw second moment of the fixed-size MICRO-batch gradients,

$$\mathbb{E}\left[\frac{1}{\kappa}\sum_{k=1}^{\kappa}g_{t-k+\kappa}^2(w_{t-\kappa})\right] = \mathbb{E}[g]^2 + \text{Var}[g] \quad (5)$$

This expectation thus does not depend on κ , avoiding a key source of batch size dependence.

4 Theorem statements

While we have clearly eliminated one source of batch size dependence, we have yet to prove that Alg. (3) really is batch size invariant in any formal sense. We begin with a theorem that states that with an appropriate choice of hyperparameters, κ steps of MICRO Adam on MICRO-batches of size M gives equivalent optimizer-state-updates (i.e. updates for m_t , v_t and g_t) to a single step of batch size invariant Adam with the same datapoints grouped into a single MINI-batch of size $B = \kappa M$ (Theorem 1). This implies that with an appropriate choice of hyperparameters, batch size invariant Adam with different MINI-batch sizes gives equivalent optimizer-state-updates after consuming the same set of data points (Theorem 2). For the proofs, see Appendices A–D.

To understand the formal statement of the theorem, we need to understand how to formally obtain small η , γ_1 and γ_2 . We do this by setting,

$$\eta = \delta\bar{\eta}_0 \quad (6a)$$

$$\gamma_1 = \delta\bar{\gamma}_1 \quad (6b)$$

$$\gamma_2 = \delta\bar{\gamma}_2. \quad (6c)$$

and taking $\delta \rightarrow 0$. Of course, as $\delta \rightarrow 0$, all state variables (w_t , m_t and v_t) stop changing so the updates from the two optimizers are trivially equivalent. To avoid this trivial equivalence, we actually consider the equivalence of weight changes, divided by δ (see below).

Theorem 1. *Consider two optimizers: MICRO Adam (Alg. 1; i.e. standard Adam applied to MICRO-batches) with hyperparameters η , γ_1 and γ_2 , and batch size invariant Adam (Alg. 3) with hyperparameters*

$$\eta' = \kappa\eta, \quad (7a)$$

$$\gamma_1' = \kappa\gamma_1, \quad (7b)$$

$$\gamma_2' = \kappa\gamma_2. \quad (7c)$$

applied to MINI-batches composed of κ MICRO-batches. We start both optimizers at time $t - \kappa$ at the same initial state, $w_{t-\kappa}$, $m_{t-\kappa}$ and $v_{t-\kappa}$. We take w_t to be the result of applying κ steps of standard Adam to κ MICRO-batches, and w'_t to be the result of applying a single step of batch size invariant Adam to a MINI-batch (consisting of the same κ MICRO-batches merged together). Then,

$$\lim_{\delta \rightarrow 0} \frac{m_t - m_{t-\kappa}}{\delta} = \lim_{\delta \rightarrow 0} \frac{m'_t - m_{t-\kappa}}{\delta} \quad (8a)$$

$$\lim_{\delta \rightarrow 0} \frac{v_t - v_{t-\kappa}}{\delta} = \lim_{\delta \rightarrow 0} \frac{v'_t - v_{t-\kappa}}{\delta} \quad (8b)$$

$$\lim_{\delta \rightarrow 0} \frac{w_t - w_{t-\kappa}}{\delta} = \lim_{\delta \rightarrow 0} \frac{w'_t - w_{t-\kappa}}{\delta}. \quad (8c)$$

i.e. the state updates for the merged and unmerged optimizers are equivalent for sufficiently small η , γ_1 and γ_2 .

Theorem 2. *Consider batch size invariant Adam under two MINI-batch sizes $B' = \kappa' M$ and $B'' = \kappa'' M$, where M denotes the size of the MICRO-batch, with hyperparameters*

$$\eta' = \kappa' \eta_0, \quad \eta'' = \kappa'' \eta_0 \quad (9a)$$

$$\gamma'_1 = \kappa' \gamma_1, \quad \gamma''_1 = \kappa'' \gamma_1 \quad (9b)$$

$$\gamma'_2 = \kappa' \gamma_2, \quad \gamma''_2 = \kappa'' \gamma_2 \quad (9c)$$

Consider an integer number of MICRO-batches, K , which can be divided by both κ' and κ'' . We start both optimizers at time $t - K$ with state $m_{t-K}, v_{t-K}, w_{t-K}$. We take K/κ' update steps with the first optimizer, which results in an optimizer state of m'_t, v'_t, w'_t . We also take K/κ'' update steps with the second optimizer, which results in an optimizer state of m''_t, v''_t, w''_t . Then,

$$\lim_{\delta \rightarrow 0} \frac{m'_t - m_{t-K}}{\delta} = \lim_{\delta \rightarrow 0} \frac{m''_t - m_{t-K}}{\delta} \quad (10a)$$

$$\lim_{\delta \rightarrow 0} \frac{v'_t - v_{t-K}}{\delta} = \lim_{\delta \rightarrow 0} \frac{v''_t - v_{t-K}}{\delta} \quad (10b)$$

$$\lim_{\delta \rightarrow 0} \frac{w'_t - w_{t-K}}{\delta} = \lim_{\delta \rightarrow 0} \frac{w''_t - w_{t-K}}{\delta}. \quad (10c)$$

i.e. the state updates are equivalent for sufficiently small η , γ_1 and γ_2 .

5 Experiments

In this section, we empirically confirmed that batch size invariant Adam with sufficiently small learning rates indeed gave almost exactly equivalent optimization results under different batch sizes. We additionally compared its optimization trajectories against standard Adam under the square root scaling rule, where we observed a higher level of inconsistency across different batch sizes.

Task description We trained ResNet-18 (He et al., 2016) and vision transformer (Dosovitskiy et al., 2020, ViT) on CIFAR-10 (Krizhevsky et al., 2009). For ResNet-18, we used standard cross-entropy loss with random cropping and flipping as data augmentation. For ViT², we used a patch size of 8 and we added QK-layernorm (Dehghani et al., 2023; Wortsman et al., 2023) for more stabilized training under larger learning rates. We additionally incorporated label smoothing loss and automatic data augmentation (Cubuk et al., 2018) to match up the test performance with the numbers reported in other literature, e.g. Schaipp et al. (2023).

Unfortunately, batchnorm itself can introduce batch size dependent effects (which arise because larger batches imply more accurate estimates of the feature means and variances). We therefore considered the ResNet-18 with batchnorm (Fig. 1) and replacing batchnorm with layernorm (Fig. 2). However, in our experiments, the dominant batch size dependent effects appeared to arise from Adam (Fig. 1), as we were able to dramatically reduce batch size dependence using our batch size invariant Adam.

Optimization setting We considered two optimization methods: Batch size invariant Adam with a MICRO-batch size of 25, with actual learning rate η' scaled linearly with the batch size B :

$$\eta' = \eta_0 B / B_{\max}, \quad (11)$$

and standard Adam, with η' proportion to \sqrt{B} :

$$\eta' = \eta_0 \sqrt{B / B_{\max}}. \quad (12)$$

²Implementation based on <https://github.com/kuangliu/pytorch-cifar/>

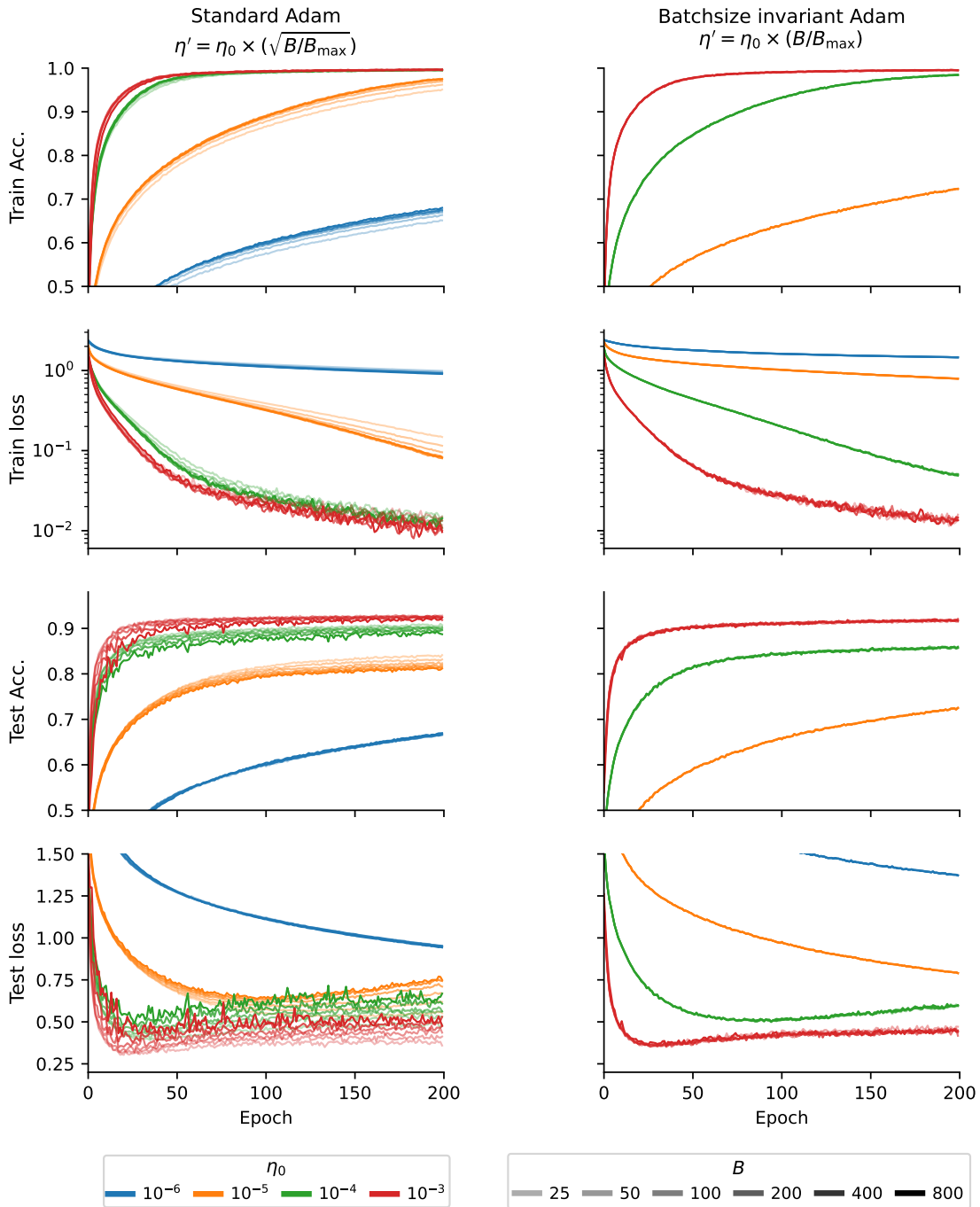


Figure 1: Comparing the behavior of our proposed batch size invariant Adam (right column), with $\eta \propto B$ against standard Adam (left column), with $\eta \propto \sqrt{B}$ (Granzio et al., 2022; Malladi et al., 2022; Hilton et al., 2022). The model was a ResNet-18 trained on CIFAR-10 over 200 epochs, under batch sizes (opacity) ranging from $B = 25$ to $B = 800$, with $B_{\max} = 800$. Each color represents a different base learning rate η_0 . Note that batch size invariant Adam (right) gives almost perfect batch size invariance (in that the lines are all on top of each other) up until $\eta = 10^{-3} \times (B/B_{\max})$. In contrast, with standard Adam (bottom), you get discrepancies even with the smallest learning rate, i.e. $\eta_0 = 10^{-6}$.

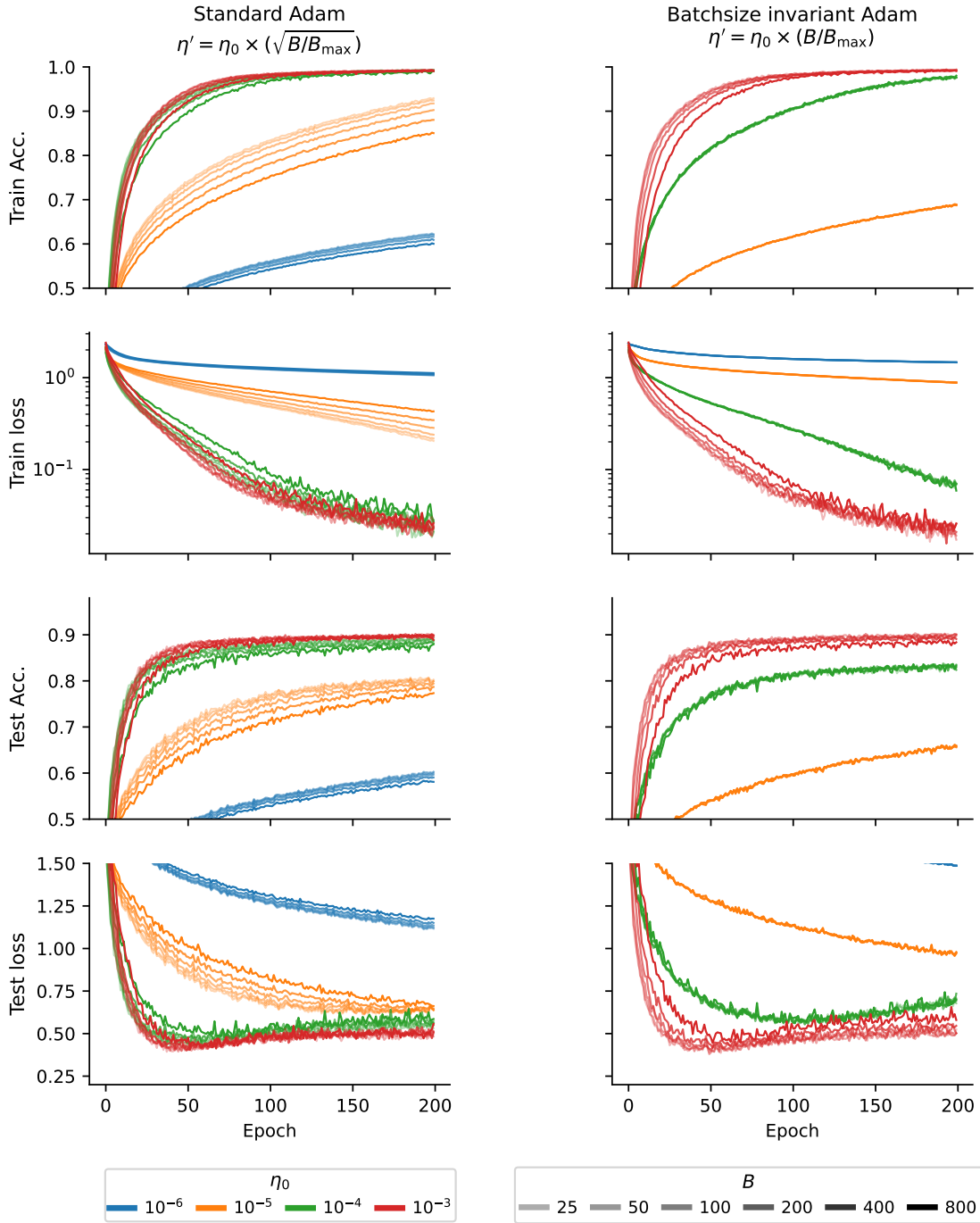


Figure 2: As Fig. 1, but with layernorm rather than batchnorm. In particular, we compare the behavior of our proposed batch size invariant Adam, with $\eta \propto B$ (right) against standard Adam, with $\eta \propto \sqrt{B}$ (left), both with $B_{\max} = 800$. Similar to the batchnorm results, the batch size invariant Adam lines (right) almost exactly line up, until $\eta = 10^{-3} \times (B/B_{\max})$. Whereas standard Adam (left) shows discrepancies between lines even under the smallest learning rate considered ($\eta_0 = 10^{-6}$).

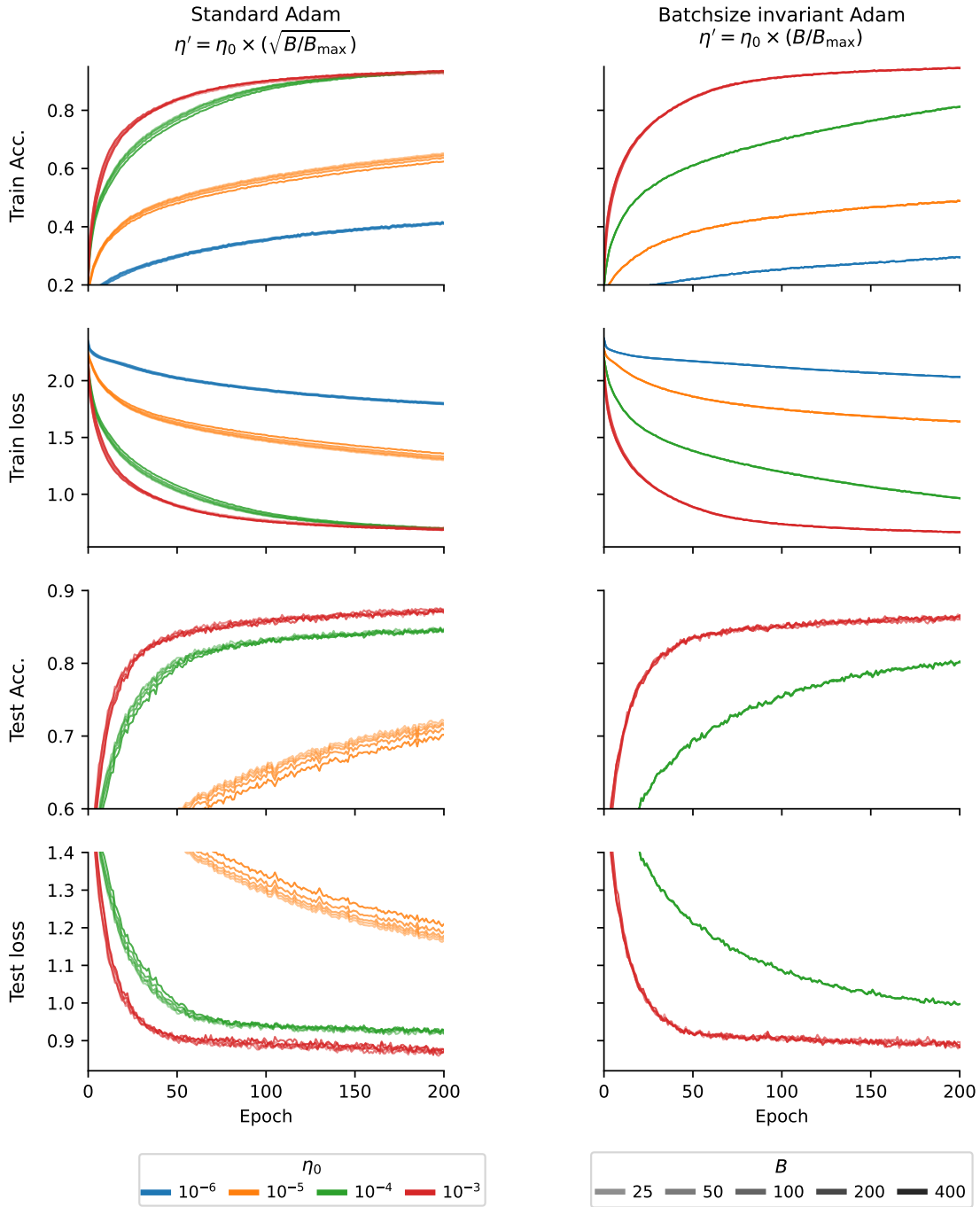


Figure 3: As Fig. 1, but use ViT rather than ResNet-18. Again, we compare the behavior of our proposed batch size invariant Adam, with $\eta \propto B$ (right) against standard Adam, with $\eta \propto \sqrt{B}$ (left). A B_{\max} of 400 is used. Standard Adam shows aligned trajectories for the smallest and largest base learning rate but shows significant discrepancy at $\eta_0 = 10^{-5}$ and in the early stage of $\eta_0 = 10^{-4}$. This is expected, as obtaining batch size invariance with standard Adam under the square-root scaling requires the gradient variance dominating the gradient mean, which may not hold when the parameters are near initialization, where the gradient may have a large magnitude. Regardless, our proposed batchsize invariant Adam shows consistency across all learning rates considered at all stages in the optimization.

where η_0 is the base learning rate and B_{\max} is the largest batch size used for a particular task. For both methods, we set the running average parameters (Hilton et al., 2022) as

$$\gamma'_1 = 0.1 \times \frac{B}{B_{\max}} \qquad \gamma'_2 = 0.001 \times \frac{B}{B_{\max}}. \quad (13)$$

For both tasks and optimizers, we experimented with η_0 in range $\{10^{-6}, 10^{-5}, 10^{-4}, 10^{-3}\}$. We tested B between 25 to 800 for ResNet and B between 25 to 400 for ViT, where the largest batch sizes (i.e. B_{\max}) are chosen as the largest value that can fit into a single 2080ti GPU. Lastly, we used constant learning rates without scheduling and no weight decay during optimization.

Results The results are presented in Fig. 1 (ResNet with batchnorm), Fig. 2 (ResNet with layernorm) and Fig. 3 (ViT). All figures show the model’s performance metrics against the training epoch for different learning rates (color) and batch sizes (opacity) averaged over three random trials.

On ResNet, under our proposed batch size invariant Adam (Fig. 1, 2 right), the trajectories under different batch sizes almost exactly overlap for all learning rates with batchnorm (Fig. 1 right), and for all except the largest learning rate with layernorm (Fig. 2 right) (note that we do expect batch size invariance to break down at some point as the learning rate increases). In contrast, the standard Adam with square-root scaling (Fig. 1 left) reveals more pronounced differences across batch sizes across a far wider range of learning rates.

Next, we considered ViT. Similar to ResNet results, our proposed batch size invariant Adam (Fig. 3 right) shows aligned trajectories across different batch sizes for all learning rates, whereas standard Adam (Fig. 3 left) shows more pronounced differences, which are especially evident for $\eta_0 = 10^{-5}, 10^{-4}$.

One thing that may be evident from the figures is that the rate of convergence for different settings of η_0 is not comparable between standard Adam and batch size-invariant Adam (i.e. comparing lines of the same color on the left and right sides of Figs. 1–3). This is expected, even for $B = B_{\max}$, so $\eta' = \eta_0$ for both standard Adam and batch size invariant Adam. The reason is that the root-mean-squared gradient denominators in the update rules are different. Standard Adam takes the average over the whole MINI-batch before computing the root-mean-squared average, which reduces the impact of variance in the gradient (Eq. (4)). In contrast, batch size invariant Adam takes the root-mean-square average for MICRO-batches (Eq. (3)), which retains contribution from variance in the gradient, even as the batch size grows.

6 Conclusions

We developed a batch size invariant Adam for large-scale distributed settings, which computes the expectation of the squared *microbatch* gradients, rather than the squared *minibatch* gradients used by standard Adam. We proved batch size invariance under mild conditions (just sufficiently small updates), without needing to go to stochastic differential equations. Furthermore, insights from (Zhang et al., 2023) suggest that this approach may even be more efficient than standard Adam in practical, large-scale settings.

References

- Cubuk, E. D., Zoph, B., Mane, D., Vasudevan, V., and Le, Q. V. Autoaugment: Learning augmentation policies from data. *arXiv preprint arXiv:1805.09501*, 2018.
- Dangel, F., Kunstner, F., and Hennig, P. BackPACK: Packing more into backprop. In *International Conference on Learning Representations*, 2020.
- Dehghani, M., Djolonga, J., Mustafa, B., Padlewski, P., Heek, J., Gilmer, J., Steiner, A. P., Caron, M., Geirhos, R., Alabdulmohsin, I., et al. Scaling vision transformers to 22 billion parameters. In *International Conference on Machine Learning*, pp. 7480–7512. PMLR, 2023.
- Dosovitskiy, A., Beyer, L., Kolesnikov, A., Weissenborn, D., Zhai, X., Unterthiner, T., Dehghani, M., Minderer, M., Heigold, G., Gelly, S., et al. An image is worth 16x16 words: Transformers for image recognition at scale. In *International Conference on Learning Representations*, 2020.

-
- Golmant, N., Vemuri, N., Yao, Z., Feinberg, V., Gholami, A., Rothauge, K., Mahoney, M. W., and Gonzalez, J. On the computational inefficiency of large batch sizes for stochastic gradient descent. *arXiv preprint arXiv:1811.12941*, 2018.
- Goyal, P., Dollár, P., Girshick, R., Noordhuis, P., Wesolowski, L., Kyrola, A., Tulloch, A., Jia, Y., and He, K. Accurate, large minibatch sgd: Training imagenet in 1 hour. *arXiv preprint arXiv:1706.02677*, 2017.
- Granzio, D., Zohren, S., and Roberts, S. Learning rates as a function of batch size: A random matrix theory approach to neural network training. *The Journal of Machine Learning Research*, 23(1):7795–7859, 2022.
- He, K., Zhang, X., Ren, S., and Sun, J. Deep residual learning for image recognition. In *Proceedings of the IEEE conference on computer vision and pattern recognition*, pp. 770–778, 2016.
- Hilton, J., Cobbe, K., and Schulman, J. Batch size-invariance for policy optimization. *Advances in Neural Information Processing Systems*, 35:17086–17098, 2022.
- Keskar, N. S., Mudigere, D., Nocedal, J., Smelyanskiy, M., and Tang, P. T. P. On large-batch training for deep learning: Generalization gap and sharp minima. *arXiv preprint arXiv:1609.04836*, 2016.
- Kingma, D. P. and Ba, J. Adam: A method for stochastic optimization. *arXiv preprint arXiv:1412.6980*, 2014.
- Krizhevsky, A. One weird trick for parallelizing convolutional neural networks. *arXiv preprint arXiv:1404.5997*, 2014.
- Krizhevsky, A., Hinton, G., et al. Learning multiple layers of features from tiny images. 2009.
- Loshchilov, I. and Hutter, F. Decoupled weight decay regularization. *arXiv preprint arXiv:1711.05101*, 2017.
- Ma, S., Bassily, R., and Belkin, M. The power of interpolation: Understanding the effectiveness of sgd in modern over-parametrized learning. In *International Conference on Machine Learning*, pp. 3325–3334. PMLR, 2018.
- Malladi, S., Lyu, K., Panigrahi, A., and Arora, S. On the sdes and scaling rules for adaptive gradient algorithms. *Advances in Neural Information Processing Systems*, 35:7697–7711, 2022.
- McCandlish, S., Kaplan, J., Amodei, D., and Team, O. D. An empirical model of large-batch training. *arXiv preprint arXiv:1812.06162*, 2018.
- Schaipp, F., Ohana, R., Eickenberg, M., Defazio, A., and Gower, R. M. Momo: Momentum models for adaptive learning rates. *arXiv preprint arXiv:2305.07583*, 2023.
- Shallue, C. J., Lee, J., Antognini, J., Sohl-Dickstein, J., Frostig, R., and Dahl, G. E. Measuring the effects of data parallelism on neural network training. *Journal of Machine Learning Research*, 20(112):1–49, 2019.
- Smith, S. L. and Le, Q. V. A bayesian perspective on generalization and stochastic gradient descent. *arXiv preprint arXiv:1710.06451*, 2017.
- Smith, S. L., Kindermans, P.-J., Ying, C., and Le, Q. V. Don’t decay the learning rate, increase the batch size. *arXiv preprint arXiv:1711.00489*, 2017.
- Stephan, M., Hoffman, M. D., Blei, D. M., et al. Stochastic gradient descent as approximate bayesian inference. *Journal of Machine Learning Research*, 18(134):1–35, 2017.
- Touvron, H., Martin, L., Stone, K., Albert, P., Almahairi, A., Babaei, Y., Bashlykov, N., Batra, S., Bhargava, P., Bhosale, S., et al. Llama 2: Open foundation and fine-tuned chat models. *arXiv preprint arXiv:2307.09288*, 2023.
- Wortsman, M., Liu, P. J., Xiao, L., Everett, K., Alemi, A., Adlam, B., Co-Reyes, J. D., Gur, I., Kumar, A., Novak, R., et al. Small-scale proxies for large-scale transformer training instabilities. *arXiv preprint arXiv:2309.14322*, 2023.

-
- Zhang, G., Li, L., Nado, Z., Martens, J., Sachdeva, S., Dahl, G., Shallue, C., and Grosse, R. B. Which algorithmic choices matter at which batch sizes? insights from a noisy quadratic model. *Advances in neural information processing systems*, 32, 2019.
- Zhang, S., Roller, S., Goyal, N., Artetxe, M., Chen, M., Chen, S., Dewan, C., Diab, M., Li, X., Lin, X. V., et al. Opt: Open pre-trained transformer language models. *arXiv preprint arXiv:2205.01068*, 2022.
- Zhang, Y., Han, Y., Cao, S., Dai, G., Miao, Y., Cao, T., Yang, F., and Xu, N. Adam accumulation to reduce memory footprints of both activations and gradients for large-scale dnn training. *arXiv preprint arXiv:2305.19982*, 2023.

A Connecting limits in Theorem 1 with gradients

Notice that the quantities in Eq. (8) can be understood as derivatives,

$$\frac{dm_t}{d\delta} = \lim_{\delta \rightarrow 0} \frac{m_t - m_{t-\kappa}}{\delta} \qquad \frac{dm'_t}{d\delta} = \lim_{\delta \rightarrow 0} \frac{m'_t - m'_{t-\kappa}}{\delta}, \quad (14a)$$

$$\frac{dv_t}{d\delta} = \lim_{\delta \rightarrow 0} \frac{v_t - v_{t-\kappa}}{\delta} \qquad \frac{dv'_t}{d\delta} = \lim_{\delta \rightarrow 0} \frac{v'_t - v'_{t-\kappa}}{\delta}, \quad (14b)$$

$$\frac{dw_t}{d\delta} = \lim_{\delta \rightarrow 0} \frac{w_t - w_{t-\kappa}}{\delta} \qquad \frac{dw'_t}{d\delta} = \lim_{\delta \rightarrow 0} \frac{w'_t - w'_{t-\kappa}}{\delta}. \quad (14c)$$

To obtain this result, we used the observation that for $\delta = 0$, the state does not change, so

$$w_t(\delta = 0) = w_{t-\kappa} \qquad w'_t(\delta = 0) = w_{t-\kappa}, \quad (15a)$$

$$m_t(\delta = 0) = m_{t-\kappa} \qquad m'_t(\delta = 0) = m_{t-\kappa}, \quad (15b)$$

$$v_t(\delta = 0) = v_{t-\kappa} \qquad v'_t(\delta = 0) = v_{t-\kappa}. \quad (15c)$$

Thus, all we need to do is show equivalence of the gradient of the state (m_t , v_t and w_t) wrt δ .

B Warmup by proving a similar result for SGD

To prove the equivalence of the merged and unmerged optimizers, it is easiest to first consider SGD. A single SGD step can be written,

$$g_t = \text{grad}_t(w_{t-1}) \quad (16a)$$

$$w_t = \text{sgd}(w_{t-1}, g_t, \eta) \quad (16b)$$

where grad_t is a function that computes the gradients for the t th microbatch, and sgd is a function that applies a single SGD update,

$$\text{grad}_t(w) = \nabla \mathcal{L}_t(w_{t-1}), \quad (17a)$$

$$\text{sgd}(w, g, \eta) = (1 - \lambda\eta)w - \eta g. \quad (17b)$$

We have written the updates in this slightly unusual form to make it possible to carefully distinguish partial and total derivatives, which turns out to be important in our setting to apply the chain rule correctly. Specifically, the chain rule applied to g_t and w_t gives,

$$\frac{dg_t}{d\eta} = \frac{\partial g_t}{\partial w_{t-1}} \frac{dw_{t-1}}{d\eta}, \quad (18a)$$

$$\frac{dw_t}{d\eta} = \frac{\partial w_t}{\partial w_{t-1}} \frac{dw_{t-1}}{d\eta} + \frac{\partial w_t}{\partial g_t} \frac{dg_t}{d\eta} + \frac{\partial w_t}{\partial \eta}. \quad (18b)$$

The partial derivatives here are formally defined as,

$$\frac{\partial g_t}{\partial w_{t-1}} = \lim_{h \rightarrow 0} \frac{\text{grad}_t(w_{t-1} + h) - \text{grad}_t(w_{t-1})}{h} \quad (19a)$$

$$\frac{\partial w_t}{\partial w_{t-1}} = \lim_{h \rightarrow 0} \frac{\text{sgd}(w_{t-1} + h, g_t, \eta) - \text{sgd}(w_{t-1}, g_t, \eta)}{h} \quad (19b)$$

$$\frac{\partial w_t}{\partial g_t} = \lim_{h \rightarrow 0} \frac{\text{sgd}(w_{t-1}, g_t + h, \eta) - \text{sgd}(w_{t-1}, g_t, \eta)}{h} \quad (19c)$$

$$\frac{\partial w_t}{\partial \eta} = \lim_{h \rightarrow 0} \frac{\text{sgd}(w_{t-1}, g_t, \eta + h) - \text{sgd}(w_{t-1}, g_t, \eta)}{h} \quad (19d)$$

i.e. the partial derivatives compute the change in the output of the *function* (either grad_t or sgd) as one of the arguments to those functions changes, while all the other arguments are held fixed. In contrast, the total

derivatives ($d/d\eta$) represent the total change through the whole “compute graph”, i.e. the total change in w_t and g_t if we start from a fixed $w_{t-\kappa}$ and change η .

To compute the total derivative for w_t , we use the following partial derivatives,

$$\frac{\partial w_t}{\partial w_{t-1}} = 1 - \lambda\eta \quad (20a)$$

$$\frac{\partial w_t}{\partial g_t} = -\eta \quad (20b)$$

$$\frac{\partial w_t}{\partial \eta} = -g_t - \lambda w_{t-1}. \quad (20c)$$

Substituting these partial derivatives into the total derivative,

$$\frac{dw_t}{d\eta} = (1 - \eta\lambda) \frac{dw_{t-1}}{d\eta} - \eta \frac{dg_t}{d\eta} - g_t - \lambda w_{t-1}. \quad (21)$$

Evaluating at $\eta = 0$,

$$\left. \frac{dw_t}{d\eta} \right|_{\eta=0} = \left. \frac{dw_{t-1}}{d\eta} \right|_{\eta=0} - g_t - \lambda w_{t-1}, \quad (22)$$

we get a simple recursive expression.

Then, if we fix $w_{t-\kappa}$, and consider computing w_t through κ steps of gradient descent, we get,

$$\left. \frac{dw_t}{d\eta} \right|_{\eta=0} = - \sum_{k=1}^{\kappa} (g_{t-\kappa+k} + \lambda w_{t-\kappa+k-1}), \quad (23)$$

We can simplify this expression by noting that at $\eta = 0$, the weights at all timesteps are equal, $w_{t-1} = w_{t-2} = \dots = w_{t-\kappa}$. This has important implications for the gradient terms. Specifically, g_t is the gradient for the t th datapoint/microbatch, evaluated using the model parameters at timestep $t - 1$, i.e. w_{t-1} . But if the weights do not change, the average of these gradients can be computed based on the initial set of weights (i.e. based on $w_{t-\kappa}$),

$$\left. \frac{1}{\kappa} \sum_{k=1}^{\kappa} g_{t-k+\kappa} \right|_{\eta=0} = \left. \frac{1}{\kappa} \sum_{k=1}^{\kappa} \text{grad}_{t-k+\kappa}(w_{t-k+\kappa-1}) \right|_{\eta=0} = \frac{1}{\kappa} \sum_{k=1}^{\kappa} \text{grad}_{t-k+\kappa}(w_{t-\kappa}) = g'_t. \quad (24)$$

Here, g'_t is this average gradient for data across all κ steps, but evaluated using the initial weights, $w_{t-\kappa}$. Thus the gradient resulting from the κ updates is,

$$\left. \frac{dw_t}{d\eta} \right|_{\eta=0} = -\kappa \lambda w_{t-\kappa} - \kappa g'_t. \quad (25)$$

This is starting to resemble a single step of a merged optimizer which performs a single step using a minibatch consisting of the κ minibatches.

However, to be sure of the connection to a single step of a merged optimizer, we need to formally define this optimizer.

$$g'_t = \text{grad}'_t(w_{t-\kappa}) \quad (26a)$$

$$w'_t = \text{sgd}(w_{t-\kappa}, g'_t, \eta') \quad (26b)$$

where grad'_t is a function that computes the gradients for the t th *minibatch*,

$$\text{grad}'_t(w) = \frac{1}{\kappa} \sum_{k=1}^{\kappa} \text{grad}_{t-k+\kappa}(w) \quad (27)$$

Now, we compute the gradient of w'_t wrt η , taking $\eta' = \kappa\eta$,

$$\left. \frac{dw'_t}{d\eta} \right|_{\eta=0} = -\kappa \lambda w_{t-\kappa} - \kappa g'_t. \quad (28)$$

This is exactly equal to the gradient wrt η of the multi-step gradient in Eq. (25), which establishes our result.

C Proof of Theorem 1

In Appendix A, we established that the limits in Theorem 1 can be understood as derivatives (Eq. 14).

However, computing gradients through multiple Adam updates is not trivial. To do so correctly, we need to be careful to distinguish partial and total derivatives. To that end, we write MICRO Adam updates (Alg. 1) (i.e. standard Adam applied to microbatches) in an unusual form,

$$g_t = \text{grad}_t(w_{t-1}) \quad (29a)$$

$$m_t = \text{ema}_1(m_{t-1}, g_t, \delta) \quad (29b)$$

$$v_t = \text{ema}_2(v_{t-1}, g_t, \delta) \quad (29c)$$

$$u_t = \text{norm_ema}_t(m_t, v_t) \quad (29d)$$

$$w_t = \text{update}(w_{t-1}, u_t, \delta) \quad (29e)$$

where,

$$\text{ema}_1(m, g, \delta) = (1 - \delta\bar{\gamma}_1)m + \delta\bar{\gamma}_1g \quad (30a)$$

$$\text{ema}_2(v, g, \delta) = (1 - \delta\bar{\gamma}_2)v + \delta\bar{\gamma}_2g^2 \quad (30b)$$

$$\text{update}(w, u, \delta) = (1 - \delta\bar{\eta}\lambda)w - \delta\bar{\eta}u. \quad (30c)$$

$$\text{norm_ema}_t(m, v) = \frac{\hat{m}_t(m)}{\sqrt{\hat{v}_t(v) + \epsilon}} \quad (30d)$$

where,

$$\hat{m}_t(m) = \frac{m}{1 - \beta_1^t} = \frac{m}{1 - (1 - \delta\bar{\gamma}_1)^t} \quad (30e)$$

$$\hat{v}_t(v) = \frac{v}{1 - \beta_2^t} = \frac{v}{1 - (1 - \delta\bar{\gamma}_2)^t} \quad (30f)$$

We are interested in the three state variables, m_t , v_t and w_t , that propagate across timesteps. Using the chain rule, the gradients for these variables can be written,

$$\frac{dm_t}{d\delta} = \frac{\partial m_t}{\partial g_t} \frac{dg_t}{d\delta} + \frac{\partial m_t}{\partial m_{t-1}} \frac{dm_{t-1}}{d\delta} + \frac{\partial m_t}{\partial \delta} \quad (31a)$$

$$\frac{dv_t}{d\delta} = \frac{\partial v_t}{\partial g_t} \frac{dg_t}{d\delta} + \frac{\partial v_t}{\partial v_{t-1}} \frac{dv_{t-1}}{d\delta} + \frac{\partial v_t}{\partial \delta} \quad (31b)$$

$$\frac{dw_t}{d\delta} = \frac{\partial w_t}{\partial w_{t-1}} \frac{dw_{t-1}}{d\delta} + \frac{\partial w_t}{\partial u_t} \frac{du_t}{d\delta} + \frac{\partial w_t}{\partial \delta} \quad (31c)$$

We begin by considering the first state variable, m_t . We substitute the partial derivatives,

$$\frac{\partial m_t}{\partial g_t} = \delta\bar{\gamma}_1 \quad (32a)$$

$$\frac{\partial m_t}{\partial m_{t-1}} = 1 - \delta\bar{\gamma}_1 \quad (32b)$$

$$\frac{\partial m_t}{\partial \delta} = \bar{\gamma}_1(g_t - m_{t-1}), \quad (32c)$$

into Eq. (31a),

$$\frac{dm_t}{d\delta} = \delta\bar{\gamma}_1 \frac{dg_t}{d\delta} + (1 - \delta\bar{\gamma}_1) \frac{dm_{t-1}}{d\delta} + \bar{\gamma}_1(g_t - m_{t-1}). \quad (33)$$

Now, we evaluate at $\delta = 0$,

$$\left. \frac{dm_t}{d\delta} \right|_{\delta=0} = \left. \frac{dm_{t-1}}{d\delta} \right|_{\delta=0} + \bar{\gamma}_1(g_t - m_{t-1}), \quad (34)$$

which gives a simple, recursive result.

We follow almost exactly the same procedure for v_t . We substitute the partial derivatives,

$$\frac{\partial v_t}{\partial g_t} = 2\delta\bar{\gamma}_2 g_t, \quad (35a)$$

$$\frac{\partial v_t}{\partial v_{t-1}} = 1 - \delta\bar{\gamma}_2, \quad (35b)$$

$$\frac{\partial v_t}{\partial \delta} = \bar{\gamma}_2(g_t^2 - v_{t-1}). \quad (35c)$$

into Eq. (31b),

$$\frac{dv_t}{d\delta} = 2\delta\bar{\gamma}_2 g_t \frac{dg_t}{d\delta} + (1 - \delta\bar{\gamma}_2) \frac{dv_{t-1}}{d\delta} + \bar{\gamma}_2(g_t^2 - v_{t-1}). \quad (36)$$

Now, we evaluate at $\delta = 0$,

$$\left. \frac{dv_t}{d\delta} \right|_{\delta=0} = \left. \frac{dv_{t-1}}{d\delta} \right|_{\delta=0} + \bar{\gamma}_2(g_t^2 - v_{t-1}), \quad (37)$$

which gives a simple, recursive result.

Finally, we follow a similar process for w_t . We substitute the partial derivatives,

$$\frac{\partial w_t}{\partial u_t} = \delta\bar{\eta} \quad (38a)$$

$$\frac{\partial w_t}{\partial w_{t-1}} = 1 - \delta\bar{\eta}\lambda \quad (38b)$$

$$\frac{\partial w_t}{\partial \delta} = -\bar{\eta}(u_t + \lambda w_{t-1}). \quad (38c)$$

into Eq. (31c),

$$\frac{dw_t}{d\delta} = \delta\bar{\eta} \frac{du_t}{d\delta} + (1 - \delta\bar{\eta}\lambda) \frac{dw_{t-1}}{d\delta} - \bar{\eta}(u_t + \lambda w_{t-1}). \quad (39)$$

Now, we evaluate at $\delta = 0$,

$$\left. \frac{dw_t}{d\delta} \right|_{\delta=0} = \left. \frac{dw_{t-1}}{d\delta} \right|_{\delta=0} - \bar{\eta}(u_t + \lambda w_{t-1}). \quad (40)$$

which gives a simple, recursive result.

Now, we consider fixing $m_{t-\kappa}$, $v_{t-\kappa}$, and $w_{t-\kappa}$ and performing κ steps of the optimizer

$$\left. \frac{dm_t}{d\delta} \right|_{\delta=0} = \bar{\gamma}_1 \sum_{k=1}^{\kappa} (g_{t-\kappa+k} - m_{t-\kappa+k-1}) \quad (41a)$$

$$\left. \frac{dv_t}{d\delta} \right|_{\delta=0} = \bar{\gamma}_2 \sum_{k=1}^{\kappa} (g_{t-\kappa+k}^2 - v_{t-\kappa+k-1}) \quad (41b)$$

$$\left. \frac{dw_t}{d\delta} \right|_{\delta=0} = -\bar{\eta} \sum_{k=1}^{\kappa} (u_{t-\kappa+k} + \lambda w_{t-\kappa+k-1}). \quad (41c)$$

Remember that as $\delta \rightarrow 0$ all the state variables do not change, and are equal to their initial values,

$$m_{t-\kappa} = m_{t-\kappa+1} = \dots = m_{t-1} = m_t \quad (42a)$$

$$v_{t-\kappa} = v_{t-\kappa+1} = \dots = v_{t-1} = v_t \quad (42b)$$

$$w_{t-\kappa} = w_{t-\kappa+1} = \dots = w_{t-1} = w_t. \quad (42c)$$

Using these constant values, along with Eq. (24),

$$\left. \frac{dm_t}{d\delta} \right|_{\delta=0} = -\kappa\bar{\gamma}_1 m_{t-\kappa} + \bar{\gamma}_1 \sum_{k=1}^{\kappa} g_{t-\kappa+k} \quad (43a)$$

$$\left. \frac{dv_t}{d\delta} \right|_{\delta=0} = -\kappa\bar{\gamma}_2 v_{t-\kappa} + \bar{\gamma}_2 \sum_{k=1}^{\kappa} g_{t-\kappa+k}^2 \quad (43b)$$

$$\left. \frac{dw_t}{d\delta} \right|_{\delta=0} = -\bar{\eta} \left(\sum_{k=1}^{\kappa} u_{t-\kappa+k} + \kappa \lambda w_{t-\kappa} \right). \quad (43c)$$

Finally, we consider the $u_{t-\kappa+k}$ terms, which requires us to consider the debiasing steps. Debiasing actually stops doing anything for fixed t , in the limit as $\delta \rightarrow 0$, (i.e. $\hat{m}_t(m) = m$). To avoid this trivial equivalence, we therefore consider a limit in which t increases as δ falls,

$$t = \bar{t}/\delta, \quad (44)$$

where \bar{t} is fixed. That makes sense, because δ decreases, all the updates become smaller, so we may want to perform more iterations. We are going to use the standard limit,

$$\lim_{x \rightarrow \infty} \left(1 + \frac{a}{x} \right)^{bx} = e^{ab}. \quad (45)$$

In particular, considering the $(1 - \bar{\gamma}_1 \delta)^t$ term in Eq. (30e), taking $t = \bar{t}/\delta$, $\delta = 1/x$, and identifying $a = -\kappa\bar{\gamma}$ and $b = \bar{t}$,

$$\lim_{\delta \rightarrow 0} (1 - \bar{\gamma}_1 \delta)^t = \lim_{x \rightarrow \infty} \left(1 - \frac{\bar{\gamma}_1}{x} \right)^{\bar{t}x} = e^{-\bar{\gamma}_1 \bar{t}}. \quad (46)$$

$$\lim_{\delta \rightarrow 0} (1 - \bar{\gamma}_2 \delta)^t = \lim_{x \rightarrow \infty} \left(1 - \frac{\bar{\gamma}_2}{x} \right)^{\bar{t}x} = e^{-\bar{\gamma}_2 \bar{t}}. \quad (47)$$

(where the second equation is exactly the same thing, but for v). In this limit, the debiasing steps can be written,

$$\lim_{\delta \rightarrow 0} \hat{m}_t(m) = e^{-\bar{\gamma}_1 \bar{t}} m, \quad (48)$$

$$\lim_{\delta \rightarrow 0} \hat{v}_t(v) = e^{-\bar{\gamma}_2 \bar{t}} v. \quad (49)$$

Substituting the result of these debiasing steps into Eq. (43),

$$\left. \frac{dm_t}{d\delta} \right|_{\delta=0} = -\kappa\bar{\gamma}_1 m_{t-\kappa} + \bar{\gamma}_1 \sum_{k=1}^{\kappa} g_{t-\kappa+k} \quad (50a)$$

$$\left. \frac{dv_t}{d\delta} \right|_{\delta=0} = -\kappa\bar{\gamma}_2 v_{t-\kappa} + \bar{\gamma}_2 \sum_{k=1}^{\kappa} g_{t-\kappa+k}^2 \quad (50b)$$

$$\left. \frac{dw_t}{d\delta} \right|_{\delta=0} = -\kappa\bar{\eta} \left(\frac{u_{t-\kappa} e^{-\bar{\gamma}_1 \bar{t}}}{\sqrt{v_{t-\kappa} e^{-\bar{\gamma}_2 \bar{t}} + \epsilon}} + \lambda w_{t-\kappa} \right). \quad (50c)$$

Overall, these updates resembles a single step of the merged, batch size invariant Adam.

But to be sure, we write batch size invariant Adam updates in Alg. (3) as,

$$g'_t = \text{grad}'_t(w_{t-\kappa}) \quad (51a)$$

$$s'_t = \text{gradsq}'_t(w_{t-\kappa}) \quad (51b)$$

$$m'_t = \text{ema}'_1(m_{t-\kappa}, g'_t, \delta) \quad (51c)$$

$$v'_t = \text{ema}'_2(v_{t-\kappa}, s'_t, \delta) \quad (51d)$$

$$u'_t = \text{norm_update}'_{t/\kappa}(m'_t, v'_t) \quad (51e)$$

$$w'_t = \text{update}'(w'_{t-1}, u'_t, \delta) \quad (51f)$$

where,

$$\text{grad}'_t(w_{t-\kappa}) = \frac{1}{\kappa} \sum_{k=1}^{\kappa} \text{grad}_{t-k+\kappa}(w_{t-\kappa}), \quad (52a)$$

$$\text{gradsq}'_t(w_{t-\kappa}) = \frac{1}{\kappa} \sum_{k=1}^{\kappa} \text{grad}_{t-k+\kappa}^2(w_{t-\kappa}), \quad (52b)$$

$$\text{ema}'_1(m, g, \delta) = (1 - \delta\kappa\bar{\gamma}_1)m + \delta\kappa\bar{\gamma}_1g \quad (52c)$$

$$\text{ema}'_2(v, s, \delta) = (1 - \delta\kappa\bar{\gamma}_2)v + \delta\kappa\bar{\gamma}_2s \quad (52d)$$

$$\text{update}'(w, u, \delta) = (1 - \delta\kappa\bar{\eta}\lambda)w - \delta\kappa\bar{\eta}u. \quad (52e)$$

$$\text{norm_update}'_{t/\kappa}(m, v) = \frac{\hat{m}'_{t/\kappa}(m)}{\sqrt{\hat{v}'_{t/\kappa}(v) + \epsilon}} \quad (52f)$$

where,

$$\hat{m}'_{t/\kappa}(m) = \frac{m}{1 - (1 - \gamma'_1)^{t/\kappa}} \quad (52g)$$

$$\hat{v}'_{t/\kappa}(v) = \frac{v}{1 - (1 - \gamma'_2)^{t/\kappa}} \quad (52h)$$

Now, the gradient of the state variables for the merged, batch size invariant Adam updates is,

$$\left. \frac{dm'_t}{d\delta} \right|_{\delta=0} = \kappa\bar{\gamma}_1 m_{t-\kappa} + \bar{\gamma}_1 \sum_{k=1}^{\kappa} g_{t-k+\kappa} \quad (53a)$$

$$\left. \frac{dv'_t}{d\delta} \right|_{\delta=0} = \kappa\bar{\gamma}_2 v_{t-\kappa} + \bar{\gamma}_2 \sum_{k=1}^{\kappa} g_{t-k+\kappa}^2 \quad (53b)$$

$$\left. \frac{dw'_t}{d\delta} \right|_{\delta=0} = -\kappa\bar{\eta}(u_t + \lambda w_{t-\kappa}). \quad (53c)$$

Comparing these expressions to Eq. (41), we are almost done. It only remains to consider κu_t , again in a limit in which t increases as δ decreases, $t = \bar{t}/\delta$. Again, we consider the $(1 - \gamma'_1)^{t/\kappa}$ term, using the standard limit, $\lim_{x \rightarrow \infty} (1 + \frac{a}{x})^{bx} = e^{ab}$, take $\delta = 1/x$, and identify $a = -\bar{\gamma}$ and $b = \bar{t}$,

$$\lim_{\delta \rightarrow 0} (1 - \gamma'_1)^{\bar{t}/(\delta\kappa)} = \lim_{\delta \rightarrow 0} (1 - \kappa\bar{\gamma}_1\delta)^{\bar{t}/(\delta\kappa)} = \lim_{x \rightarrow \infty} (1 - \frac{\kappa\bar{\gamma}_1}{x})^{\frac{\bar{t}}{\kappa}x} = e^{-\bar{\gamma}_1\bar{t}}. \quad (54)$$

Thus, the debiasing steps can be written,

$$\lim_{\delta \rightarrow 0} \hat{m}'_{t/\kappa}(m) = e^{-\bar{\gamma}_1\bar{t}}m, \quad (55a)$$

$$\lim_{\delta \rightarrow 0} \hat{v}'_{t/\kappa}(v) = e^{-\bar{\gamma}_2\bar{t}}v. \quad (55b)$$

Which gives final gradients,

$$\left. \frac{dm'_t}{d\delta} \right|_{\delta=0} = -\kappa\bar{\gamma}_1 m_{t-\kappa} + \bar{\gamma}_1 \sum_{k=1}^{\kappa} g_{t-\kappa+k} \quad (56a)$$

$$\left. \frac{dv'_t}{d\delta} \right|_{\delta=0} = -\kappa\bar{\gamma}_2 v_{t-\kappa} + \bar{\gamma}_2 \sum_{k=1}^{\kappa} g_{t-\kappa+k}^2 \quad (56b)$$

$$\left. \frac{dw'_t}{d\delta} \right|_{\delta=0} = -\kappa\bar{\eta} \left(\frac{u_{t-\kappa} e^{-\bar{\gamma}_1\bar{t}}}{\sqrt{v_{t-\kappa} e^{-\bar{\gamma}_2\bar{t}} + \epsilon}} + \lambda w_{t-\kappa} \right). \quad (56c)$$

These gradients are exactly the same as the gradients for the multi-step updates (Eq. 41), which proves our result.

D Proof of Theorem 2

By Theorem 1,

$$\lim_{\delta \rightarrow 0} \frac{w'_t - w_{t-K}}{\delta} = \lim_{\delta \rightarrow 0} \frac{w_t - w_{t-K}}{\delta} = \lim_{\delta \rightarrow 0} \frac{w''_t - w_{t-K}}{\delta} \quad (57a)$$

$$\lim_{\delta \rightarrow 0} \frac{m'_t - m_{t-K}}{\delta} = \lim_{\delta \rightarrow 0} \frac{m_t - m_{t-K}}{\delta} = \lim_{\delta \rightarrow 0} \frac{m''_t - m_{t-K}}{\delta} \quad (57b)$$

$$\lim_{\delta \rightarrow 0} \frac{v'_t - v_{t-K}}{\delta} = \lim_{\delta \rightarrow 0} \frac{v_t - v_{t-K}}{\delta} = \lim_{\delta \rightarrow 0} \frac{v''_t - v_{t-K}}{\delta}. \quad (57c)$$

where m_t, v_t, w_t is the result of applying K steps of Micro-Adam, with hyperparameters η, γ_1, γ_2 .